# A new image processing method for extracting integrated intensities from low-energy electron diffraction spots

Jahansooz Toofan and Philip R. Watson
*Department of Chemistry and Center for Advanced Materials Research, Gilbert Hall 153, Oregon State University, Corvallis, Oregon 97331-4003*

(Received 7 April 1994; accepted for publication 26 July 1994)

We have devised and programmed a new scheme based on image processing techniques for extracting the intensity of fluorescent display low-energy electron diffraction spots. The method make no assumptions about spot shape, does not use thresholding, and can deal with badly behaved backgrounds, noise spikes, and dead pixels. All decisions about whether a particular pixel belongs to a spot or to the background are made on purely logical grounds with generally binary operator masks. Once the spot edge has been defined, a local background is subtracted to generate an integrated spot intensity. Extensive tests with diffraction features ranging from very strong to indistinguishable from background by eye show this method to be stable, fast, and reproducible.

## I. INTRODUCTION

Low-energy electron diffraction (LEED) has proved to be one of the most successful techniques for the quantitative determination of the structure of surfaces.[1] The most usual approach is to record the intensities of the diffracted LEED beams as a function of the energy of the electron beam to generate intensity-voltage, or $I$-$V$, curves. The experimental data is then compared with the corresponding theoretical curves calculated for an assumed surface structure, and the best fit from various surface geometries determined via a suitable reliability factor. The crucial experimental requirement is to be able to record the diffracted intensities reliably and quickly in order to avoid contamination or decomposition on the surface. Data collection by Faraday cup meets the first requirement, but not the second, and is exceedingly tedious if it is desired to collect data from a large number of beams. In most LEED systems the diffracted beams are displayed as "spots" on a fluorescent screen. The data from such displays can be quickly collected by either photographing to film and analyzing off-line,[2] or recording the image of the screen with a TV camera and extracting the intensity of the spots on-line[3–5] or off-line.[6–9] The recent digital LEED approach[10,11] records the screen image directly to disk with a multichannel-plate/resistive anode.

The common feature of all the approaches to LEED data collection that record the whole screen image is the need to extract the integrated intensity from the pixels within a spot while accurately subtracting the background intensity from the fluorescent screen underlying the spot. Previous workers in this area have ignored background contributions to the spot[5] or used simple thresholding techniques to extract the integrated spot intensities. Carvalho *et al.*[7] assume a Gaussian shape of the spot and take the spot radius to be the full width at half-maximum. Tommet *et al.*[4] point out that LEED spots are more properly regarded as Lorentzian in shape and used an arbitrary definition of the spot size based on estimates of "typical" or "maximum" spot sizes, as have many others.[2,3,6,8] However, regardless of the way in which the size of the spot is determined, all these methods assume the spot to be circular in cross section and measure an average background from a circular area around the spot. This value then sets the threshold above which a pixel is counted as part of the spot.

Such threshold approaches have the merit of simplicity but can easily lead to incorrect integrations if the spot has a noncircular cross section. Also, preferably, the local threshold needs to be redefined for each spot. Unfortunately, in many cases the diffracted spots may have nonideal shapes due to defects in the screen phosphor, poorly compensated magnetic fields, Moire patterns from grids, or the presence of disorder in a particular crystallographic direction. In addition, if the background is nonuniform the threshold may be incorrectly set, resulting in poor estimates of the intensities. In reality the screen response can be substantially *nonuniform* and areas of the screen or camera may be "dead," producing anomalously low or zero intensity. Sometimes field emission from sharp whiskers on the retarding grids can produce very sharp bright spots that are not part of the diffraction pattern. Weak spots with a substantial noise component can be particularly difficult to treat.

We present here a new method to extract the intensity of LEED spots that have been recorded in a digital format as a whole screen image. This approach uses some of the ideas that have been successfully used in image processing applications.[12–15] This method obviates the need to set *any* kind of background threshold (global or local) which makes it entirely general for any type of background. Furthermore, no assumptions are made about spot shape and we also automatically account in a reasonable way for anomalous intensities, such as "dead pixels." This methodology is not restricted to the analysis of LEED spots but could be applied to quite different applications such as astronomy.

## II. EXPERIMENTAL DETAILS

The LEED data itself is recorded using a COHU silicon-intensified low-light level camera. An image processing board (Coreco OC200), housed in IBM-compatible computer, produces a 512×480 7-bit image of the diffraction spots at some electron-beam energy that is stored directly on the computer hard disk using a data-collection routine writ-

 0034-6748/94/65(11)/3382/7/$6.00 

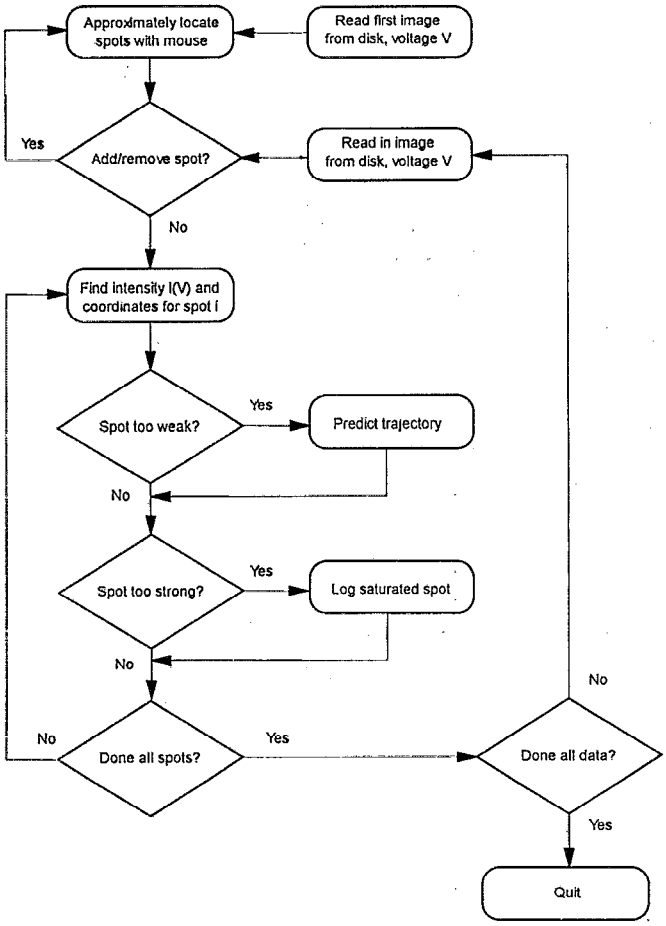


FIG. 1. General scheme of analysis for a dataset stored on disk.

ten in MicroSoft "QUICK C." The voltage of the electron beam is set via a D/A card (Metrabyte DASH-8) that sends pulses to a home-built motor controller. The stepper motor is directly connected to the beam voltage potentiometer of the LEED gun controller (Varian 981-2145). The electron-beam voltage and current are read (after filtering) from the rear monitor jacks on the controller using the same D/A card. These values are used to adjust the current to a specified value and are recorded in a file for future use. Data at one voltage can be collected and stored in about 2 s.

## III. ANALYSIS METHOD

A separate analysis program is used to automatically bring up each image in turn and extract the integrated, background-corrected intensities of the LEED spots at a specific beam voltage. These intensities are written to file for each frame resulting in a set of intensity-voltage ($I$-$V$) data.

There are a number of features of this sort of analysis that can cause difficulties and necessitated a high degree of flexibility in the design of this code (Fig. 1). In particular, spots appear and disappear as a function of beam voltage. In order to produce the complete $I$-$V$ curves we have to ensure that spots are not "lost," or confused with others. This is done using a predictor-corrector algorithm. We also allow for the number of spots being analyzed to be dynamically adjusted during a run.

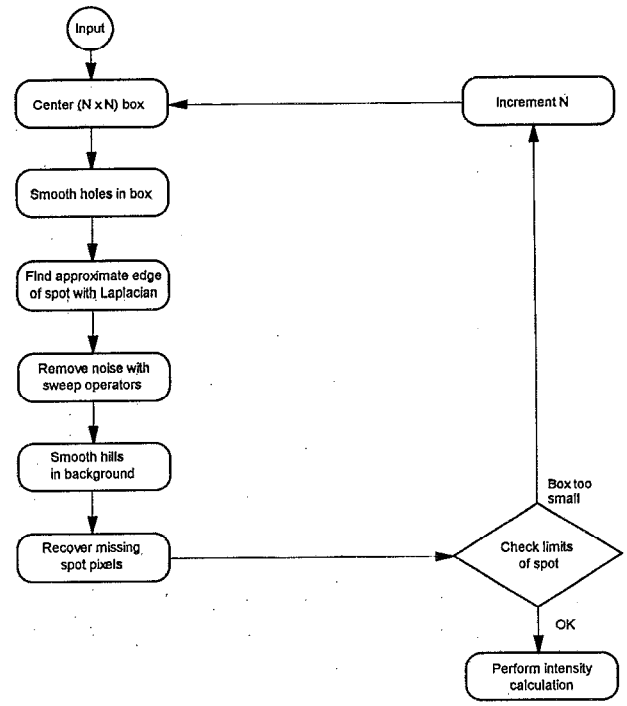


FIG. 2. Scheme of spot intensity analysis.

The process of finding the integrated spot intensity uses a number of image-processing operators that automatically find a reasonable approximation of the spot, no matter how unusual its shape may be. They also remove noise spikes and other nonphysical intensity variations. These operators are defined in the Appendix; we should note that we have on occasion constructed operators in nonstandard forms to best fit our application.

The flow of the analysis process for determining the intensity of a single spot is laid out in Fig. 2. This flowsheet is simplified by omission of some extra noise-removal steps to improve readability. Once a spot has been approximately located using the mouse, it is centered on the center of gravity of this region in an odd-dimensioned ($N\times N$) pixel box. The size of this box is initially chosen by the operator but is dynamically varied by the program to best fit the data. If the diffraction spot that we eventually recover from the data extends to within 2 pixels of the box borders, the box is deemed to be too small and we increment the box dimensions and loop back to the beginning of the analysis. The analysis is repeated until the spot fits inside an ($N-2\times N-2$) area inside the box. We find that the box dimensions do not need to exceed ($19\times 19$) for most situations.

### A. Initial estimation of the spot

The problem of extracting local areas of high intensity from background is a well-known problem in image processing. Techniques that have been employed include intensity histogramming followed by thresholding,[16] textural thresholding using Laplacian, Sobel, or other operators,[16] the use of rank operators such as the top-hat operator,[17] and pixel-tree clipping.[18] We have chosen to use a type of Laplacian operator to record the approximate extent of the diffraction spot. This operator rapidly and reproducibly produces an ap-

proximate location of a group of high intensity pixels with no constraints in terms of predefined sizes or intensity levels. However, it does result in some error in that some pixels that should be in the spot are lost. We recover these pixels and refine the size of the spot with other operators described below.

The crucial task is to sort those pixels into those that belong to the LEED diffraction spot—a spot pixel $P^s$— and those that belong to the area outside the spot—a background pixel $P^b$. Our Laplacian-type operator has a special shape that allows it to perform a second-order spatial differentiation in the horizontal, vertical, and diagonal directions. The operator is used in the form of a mask with elements that is passed over each location within an operating window $(3 \leqslant i,j \leqslant N-2)$ inside the original $(N \times N)$ frame of data (see Appendix for descriptions of this and the other operators).

The actual values that result from the use of the Laplacian are not in themselves very useful; what is important is where they change sign. Hence we use this operator in a normalized form that produces a binary image of the spot and background. A copy of the original data matrix is made in which pixels where the local value of the second derivative is negative are assigned a value of 1 (colloquially called "ON" pixels) and pixels where the local derivative is zero or positive are assigned a value of 0 ("OFF" pixels). The result is the diffraction spot being imaged as ON values in a background of mainly OFF values. We define a spot as containing at a minimum a $(3 \times 3)$ contiguous cell of ON values in the matrix obtained after using the normalized Laplacian operator.

The Laplacian operator is very sensitive to the presence of "holes"—that is, pixels with anomalously low intensity values compared to the other pixels in its vicinity (as might occur due to a dead area of screen phosphor). Such holes can disrupt the action of the Laplacian in defining the diffraction spot, so before applying this operator we first find such defects and replace their intensity values with an average of the surrounding pixels using a smoothing operator.

### B. Spot refinement

We next remove small high-intensity areas in the background that are not part of the spot using a type of morphological[19] operator that we term a "sweep operator." It sweeps through the normalized Laplacian matrix searching for single, or small groups, of ON pixels that are not part of a spot cell. These are interpreted as unwanted spikes in the image and such pixels are converted to OFF pixels. We assume that the edge of the spot should be a smooth feature within the resolution of the pixels used to define the image. The application of the Laplacian and sweep operators can result in the edge of the spot being eroded; that is, they introduce defects and holes in the edge that make it unsmooth. We therefore use another morphological[19] operator we term "recovery operators" to rectify such errors. These operators search in the vicinity of the current edge of the spot, i.e., along the outer set of ON pixels, for adjacent OFF pixels. The two operators test if such an OFF pixel is logically located in what may be a defect or hole in the true edge of the spot. This criterion alone is not enough to decide whether or not a particular OFF pixel should be included in the spot. We further require that its grayscale value exceeds a value $P_{\text{edge}}$ that represents a reasonable estimate of the local background level. If both of these conditions are passed, the pixel is considered to actually belong to the spot and is reassigned as ON.

The recovery operators need the conditional value $P_{\text{edge}}$ derived from the background to decide whether a pixel belongs to the spot or not. We have tried several approaches to fixing this quantity. We find that using a single $P_{\text{edge}}$ value for the whole array results in poor edge recovery when the background varies substantially from one side of the spot to the other. Rather, we split the frame into quadrants, where each quadrant overlaps its neighbor by one row or column, in order that the value of $P_{\text{edge}}(q)(q = 1,4)$ represents a more local value. The question still remains as to what the local value of this quantity should be. Using the average background value in the quadrant $P^b_{\text{avg}}(q)$ results in many pixels being added to the spot edge and the spot dimensions growing unreasonably large. On the other hand, using the largest pixel value in that quadrant's background—$P^b_{\text{max}}(q)$—results in too weak a recovery action. If the background values obeyed a normal distribution then we could bin the background values and use a statistical measure, e.g., $2\sigma$, to set $P_{\text{edge}}$. Unfortunately, the background values are closely grouped within a few pixel values and this approach is not feasible. The compromise value (having first smoothed out any anomalously high intensity areas in the background) that we have found to be the most stable and useful is

$$P_{\text{edge}}(q) = \frac{P^b_{\text{max}}(q) + P^b_{\text{avg}}(q)}{2}.$$

We have also found that we need to exercise particular care when dealing with values like averages and quantities such as $P_{\text{edge}}$ that employ a divisor. When we divide the integer pixel values we have to take care over whether we round up or down in order to preserve the correct relationship between quantities. For instance, incorrect rounding could result in the expression of $P_{\text{edge}}$ wrongly being set to the background maximum rather than somewhat below it.

### C. Intensity calculation

Once we have defined which pixels belong to the spot $(P^s)$ and those that belong to the background outside the spot $(P^b)$, all that remains is to integrate the intensity of the spot within the edge while accurately subtracting the local background intensity under the spot. Unfortunately, we only know the values of the background pixels outside the spot, not the background that underlies the spot. Some workers perform a two-dimensional polynomial fit of the $P^b$ pixels[16] and then interpolate the background under the spot. We have not at this time pursued this idea because of impact on the speed of analysis and the programming overhead involved.

At present we are using a simple procedure that appears to give excellent results. We use the argument that if we have correctly located the spot, then the hidden background under any quadrant of the spot must be similar to the average back-

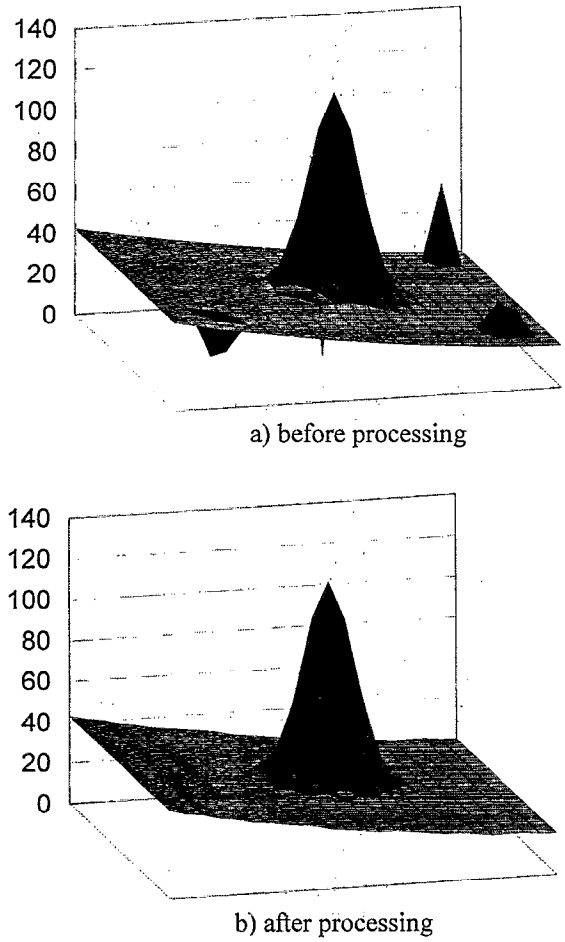


FIG. 3. Three-dimensional plot of the intensity distribution of (a) an artificial "spot" based on a Gaussian distribution on a nonlinear background with defects and (b) the result of processing the data in (a). The solid line in (b) indicates the boundary of the spot as found by our algorithm.

ground value in that quadrant. We have already used the calculated quantity $P^b_{\text{avg}}(q)$ and so we further use this value as the local background under the spot pixels in that quadrant. We therefore subtract this local background from each spot pixel and calculate the integrated background-subtracted intensity in each quadrant. The sum over the four quadrants is then normalized to unit beam current by division by the electron-beam current $i_b$ to give the final spot intensity for spot $k$ at voltage $V$, $I_k(V)$:

$$I_k(V)=\frac{1}{i_b}\sum_{q=1}^{4}\left(\sum_{i=1}^{N(q)}\sum_{j=1}^{N(q)}[P^s_{ij}(q)-P^b_{\text{avg}}(q)]\right).$$

## IV. EXAMPLES OF USE

We have extensively tested our method in two ways. The first was to construct artificial datasets that test the limits of the method. Having convinced ourselves that the codes successfully handle these, we then tested the method on real data.

As an example of the use of the method with an artificial dataset, we show in Fig. 3(a) a "spot" constructed from a Gaussian that sits on a nonlinear background. We have deliberately placed a low intensity hole in the spot itself as well

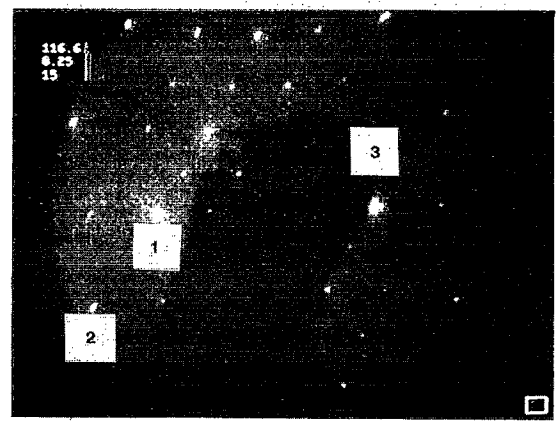


FIG. 4. Photograph of the LEED pattern from the Mo(110) $p(2\times2)$-S structure at 116.6 V beam voltage. The numbers 1–3 label diffraction spots (immediately above the labels) that have strong, medium, and weak intensity at this voltage. The quality of the original is much higher than this reproduction taken with a screen capture device of limited resolution (Polaroid Freezeframe).

a sharp noise spike and other high and low intensity area problems in the background. Figure 3(b) shows the end result of applying our method to this dataset. It is clear that we have successfully removed the spike and the other features in the area outside of the spot. This is necessary to estimate the background accurately. The program has also successfully repaired the hole in the spot. Such artifacts need to be removed to perform the integration properly. The spot is correctly placed on the sloping background—the border of the spot does not include a large portion of background that would result from the application of a simple threshold value to define the spot.

We further tested the method on a set of LEED data from the 0.25 monolayer $p(2\times2)$ structure formed by sulfur on

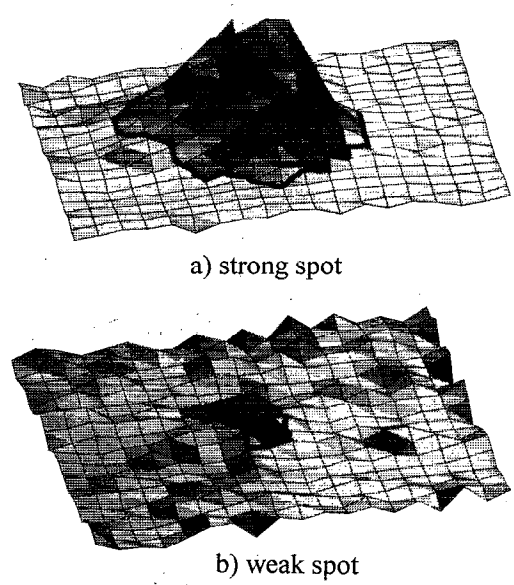


FIG. 5. Three-dimensional plot of the intensity distribution after processing about (a) an intense spot (1 in Fig. 3) and (b) a weak spot (3 in Fig. 3). The solid lines indicate the boundary of the spot as found by our algorithm.

TABLE I. Statistical summary of the operation of the image processing scheme on a strong and a weak diffraction spot (1 and 3, respectively, in Fig. 3). Shown are the number of pixels in the spot and the difference between the average grayscale values of spot and background pixels (Δavg), the percentage change in the total of the grayscale values before and after processing (%Δg), and the final integrated spot intensity (not normalized to unit beam current).

| Type of spot | No. of pixels in spot | No. of pixels in background | Δavg (avg. spot-avg. backg) | %Δg (Σ final−Σ original) | Integrated spot intensity |
|---|---|---|---|---|---|
| Strong | 54 | 307 | 37.0 | −0.27 | 2038.0 |
| Weak | 16 | 345 | 3.1 | −0.87 | 59.0 |

the (110) face of Mo. The experiment yielded over 20 different $I$-$V$ curves for two angles of incidence which was used to determine the adsorption site and bond distances to the S, as well as small rearrangements of the underlying Mo atoms.[20] The spots fall into the two classes—integral order spots of relatively high intensity, although the $I$-$V$ curves show considerable structure, and half-order spots that are generally weak. Figure 4 shows the LEED pattern at 116.6 V beam voltage. At this voltage spots vary in intensity from weak half-order spots (3) to medium (2) or strong (1) integral order spots. It is also apparent that the background is nonuniform and that some spots show some asymmetry, e.g., spot 2.

Figure 5 and Table I show the results of the analysis for spots 1 and 3. The strong spot 1 occupies about one quarter of the frame area. This spot is clearly asymmetric, there being a significantly longer tail to the left, as viewed in Fig. 5(a), than to the right. In addition, the top of the peak appears to have some structure, possibly due to a retarding-grid Moiré pattern effect. Our approach has no difficulty dealing with these problems. The average intensity in the spot is about 37 intensity units higher than the background and the integrated intensity of 2038.0 reflects the high intensity of this spot. The solid line in Fig. 5(a) showing the limit of the spot as defined by these routines is a good approximation to separating the spot from the background. Figure 5(b) shows the result of the analysis for the very weak feature 3 in Fig. 4. It is so weak as to be essentially invisible to the naked eye at this voltage, yet our routines successfully locate it. The spot covers only about 4% of the pixels and has an intensity of only about 3% of spot 1, being only about 3 intensity units above background on average. The penultimate column of Table I contains the percentage by which the total value of all the grayscale pixel values has changed during the analysis. This fraction is very small, which means that the smoothing operations have not made major changes to the original grayscale distribution, i.e., we are not overmanipulating the data.

Figure 6 shows the complete $I$-$V$ curves for the three spots shown in Fig. 4. Each curve has its own distinctive structure that we take advantage of in a structural analysis. We expect the curves to be smooth with no sharp dips or spikes. The results of our analysis bear this out even for the very weak beam 3 which shows no anomalous spikes in the low intensity areas, e.g., close to 100 V. The structure between 170 and 200 V for beam 2, though weak, is reproducible.

The principle advantages of our method is the avoidance of any arbitrary local or global thresholds to define a spot. We illustrate this point in Fig. 7 where we compare the $I$-$V$ curves that result for spot 1 from using our algorithm with those from global thresholding at two values. Because the spot moves across the screen, it hence samples different backgrounds, and changes its intensity markedly as the voltage is changed. As a result we might expect a global threshold (of any value) to give good results at some voltages and poor results at others. We can see that below about 175 V the two threshold curves bracket our data, although the low threshold is closer to our data in some areas, e.g., near 90 V and the higher threshold is closer to our data at other points,

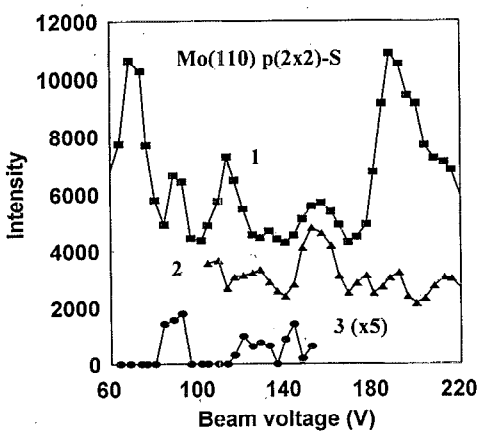


FIG. 6. Intensity-voltage curves for the three spots marked in Fig. 3. Curves 1 and 2 have been displaced vertically by 4000 and 2000 units, respectively, for clarity.

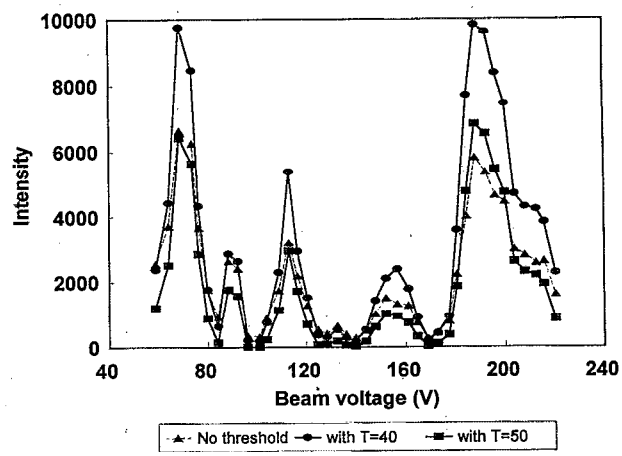


FIG. 7. Intensity-voltage curves for the spot 1 marked in Fig. 3—(a) with a global threshold of 40 intensity units, (b) with a global threshold of 50 units, and (c) for our method. The curves have been displaced vertically for clarity.

e.g., near 70 and 110 V. The principal difference between the curves occurs above 180 V where both thresholding curves lie above our data. We attribute this to the inability of such thresholds to successfully cope with the increased background at high voltages caused by the presence of more inelastically scattered electrons. As a result, thresholds overestimate the spot intensity at these high voltages, whereas our method dynamically adjusts to the changing backgrounds conditions and more correctly defines the diffraction spot.

## APPENDIX

Our procedures involve image processing operations that can operate on one of two types of data array. One type of array is the original frame of $(N\times N)$ original grayscale pixels values $P_{ij}(i,j=1,N)$. The other type of data array is an $(N\times N)$ array of binary pixel values $L_{ij}=0$ or 1 $(i,j=3,N-2)$ that result from the application of the Laplacian operator, hence the use of $L$. These define whether a particular pixel is part of a diffraction spot or not.

We use the following definitions:

(1) ON/OFF pixel—a pixel assigned a value $L_{ij}=1/0$.
(2) Cell—a $(3\times3)$ square arrangement of ON pixels. The sum of the $L$ pixel values if 9 and defines the minimum size for recognition of the presence of a spot.

The operators we employ are used to making decisions about the nature of a test pixel located at position $(ij)$ in the original data array. They take the form of a square mask of odd dimension $(M\times M)$ with elements $M_{mn}$ which are passed over the frame starting in the top left corner with the following characteristics:

(1) Mask elements: $M_{mn}$, where $m=[i+r-(M+1)/2]$ and $n=[i+s-(M+1)/2]$ for $r$ and $s=1,...,M$.
(2) Test element: the central element of the mask $M_{mn}=M_{ij}$ maps to the location of the test pixel $P_{ij}$ (or $L_{ij}$) in an $(N\times N)$ frame.
(3) Counter elements: the mask elements $M_{mn}=1$ $(m\neq i,n\neq j)$ surrounding the test element that contribute to the testing process (not all possible elements are necessarily used).
(4) Size: the number of counter elements.
(5) Switch value: a number that is used conditionally to decide whether the test pixel value should be changed (shown at top right corner of mask).

Below we define the operators we have used. They have been optimized for our purposes and in some cases differ slightly from standard forms. In order to clarify discussion we have coined our own names for each operator.

### 1. Laplacian-type operator

We use a variant of this type of operator[16] which defines the curvature in the neighborhood of the test pixel using original grayscale values $P_{ij}$ and produces a set of binary pixel values $L_{ij}$ via a $(5\times5)$ mask:

Laplacian operator mask:

$$M=\begin{vmatrix} +1 & 0 & +1 & 0 & +1 \\ 0 & +1 & +1 & +1 & 0 \\ +1 & +1 & -16 & +1 & +1 \\ 0 & +1 & +1 & +1 & 0 \\ +1 & 0 & +1 & 0 & +1 \end{vmatrix},$$

for test pixel $P_{ij}$,

$$L_{ij}=\sum_{r=1}^{5}\sum_{s=1}^{5}(P_{mn}M_{mn}),$$

and then

$$L_{ij}=1 \quad \text{if } L_{ij}<0 \quad \text{or } L_{ij}=0 \quad \text{if } L_{ij}\geqslant 0.$$

### 2. Smoothing operator

Only pixels that are anomalously high or low in intensity compared to their eight neighbors are replaced by an average of these neighboring pixel values using a $(3\times3)$ mask:

Smoothing operator mask:

$$M=\begin{vmatrix} +1 & +1 & +1 \\ +1 & 0 & +1 \\ +1 & +1 & +1 \end{vmatrix}^{>6},$$

if $(P_{mn}-P_{ij})M_{mn}\neq 0$, then $N_c=N_c+1$; then if

$$\sum_{c=1}^{8}N_c>6, \quad P_{ij}=\sum_{r=1}^{3}\sum_{s=1}^{3}(P_{mn}M_{mn})/8.$$

### 3. Sweep operator

This operator removes groups of high intensity pixels in the background due to, e.g., field-emission spikes. For an ON test pixel of interest at position $(ij)$ in the binary $L$ array, this operator counts the ON pixels in the 24 pixels that surround it in a binary $(5\times5)$ array. If this sum $S_{ij}$ is less than 8—the value for a cell—then the ON pixel in question is deemed to not be part of a spot and is turned OFF $(L_j=0)$:

Sweep operator mask:

$$M=\begin{vmatrix} +1 & +1 & +1 & +1 & +1 \\ +1 & +1 & +1 & +1 & +1 \\ +1 & +1 & 0 & +1 & +1 \\ +1 & +1 & +1 & +1 & +1 \\ +1 & +1 & +1 & +1 & +1 \end{vmatrix}^{<8}_{24},$$

if $L_{ij}=1$ (ON) and if

$$S_{ij}=\sum_{r=1}^{5}\sum_{s=1}^{5}(L_{mn}M_{mn})<8,$$

then

$$L_{ij}=0 \quad \text{(OFF)}.$$

## 4. Recovery operator

These operators employ connectivity arguments[17] about the spot boundary to decide whether a pixel that is currently in the background and is therefore not included in the spot should in fact be included. The two operators test whether an OFF test pixel is logically part of the edge of the spot or not. To be included in the spot the test pixel also has to a have an intensity value greater or equal to the test value $P_{\text{edge}}(q)$:

Recovery operator masks:

$$M_1=\begin{vmatrix} 0 & +1 & 0 \\ +1 & 0 & +1 \\ 0 & +1 & 0 \end{vmatrix}^{>1}$$

and

$$M_2=\begin{vmatrix} +1 & 0 & +1 \\ 0 & 0 & 0 \\ +1 & 0 & +1 \end{vmatrix}^{\geqslant 1},$$

for $L_{ij}=0(\text{OFF})$, if

$$C=\sum_{r=1}^{3}\sum_{s=1}^{3}(L_{mn}M_{mn})>\text{switch value},$$

and if $P_{ij}\geqslant P_{\text{edge}}(q)$, then $L_{ij}=1(\text{ON})$.


[1] P. R. Watson, J. Phys. Chem. Ref. Data **16**, 953 (1987).
[2] P. C. Stair, G. J. Kaminska, L. L. Kesmodel, and G. A. Somorjai, Phys. Rev. B **11**, 623 (1975).
[3] D. C. Frost, K. A. R. Mitchell, F. R. Shepherd, and P. R. Watson, J. Vac. Sci. Technol. **13**, 1196 (1976).
[4] T. N. Tommet, G. B. Olszewski, P. A. Chadwick, and S. L. Bernasek, Rev. Sci. Instrum. **50**, 147 (1979).
[5] H. Leonhard, A. Gutmann, and K. Hayek, J. Phys. E **13**, 298 (1980).
[6] P. Heilman, E. Lang, K. Heinz, and K. Muller, Appl. Phys. **9**, 247 (1976).
[7] V. E. Carvalho, M. W. Cook, P. G. Cowell, O. S. Heavens, M. Prutton, and S. P. Tear, Vacuum **34**, 893 (1984).
[8] T. Guo, R. E. Atkinson, and W. K. Ford, Rev. Sci. Instrum. **61**, 968 (1990).
[9] P. C. Stair, Rev. Sci. Instrum. **51**, 132 (1980).
[10] E. G. McRae, R. A. Malic, and D. A. Kapilow, Rev. Sci. Instrum. **56**, 2077 (1985).
[11] D. F. Ogletree, G. S. Blackman, R. Q. Hwang, U. Starke, and G. A. Somorjai, Rev. Sci. Instrum. **63**, 102 (1992).
[12] L. J. Galbiati, *Machine Vision and Digital Image Processing Fundamentals* (Prentice-Hall, Englewood Cliffs, NJ, 1990).
[13] E. Masakazu, *Machine Vision, A Practical Technology for Advanced Image Processing* (Gordon and Breach, New York, 1989).
[14] I. Overington, *Computer Vision* (Elsevier, Amsterdam, 1992).
[15] J. C. Russ, *The Image Processing Handbook* (CRC, Boca Raton, 1992).
[16] J. C. Russ, *The Image Processing Handbook* (CRC, Boca Raton, 1992), p. 113.
[17] D. S. Bright and E. B. Steel, in *Microbeam Analysis*, edited by A. D. Romig and W. F. Chambers (San Francisco Press, San Francisco, 1986), p. 517.
[18] R. C. Gonzales and P. Wintz, *Digital Image Processing* (Addison-Wesley, Reading, MA, 1987).
[19] J. Serra, *Image Analysis and Mathematical Morphology* (Academic, London, 1982).
[20] J. Toofan, G. Tinseth, and P. R. Watson, J. Vac. Sci. Technol. A **12**, 224 (1994).